Preprints of the 21st IFAC World Congress (Virtual)
Berlin, Germany, July 12-17, 2020

Hybrid Controller with Fuzzy Logic Technique for Three Phase Half Bridge Interleaved Buck Shunt Active Power Filter

S. Echalih*, A. Abouloifa*, J. M. Janik, I. Lachkar***, Z. Hekss*, F. Z. Chaoui****, F. Giri****

*TI Lab, Faculty of sciences Ben M'sik, Hassan II University of Casablanca, BP 7955 Casablanca, Morocco (Tel: +212682225112; e-mail: salwa.echalih-etu@etu.univh2c.ma).
**Normandie UNIV, UNICAEN, ENSICAEN, LAC, 14000 Caen, France
***ESE Lab, ENSEM, Hassan II University of Casablanca, BP 8118 Casablanca, Morocco.
****LMP2I Lab, ENSET, Mohammed V University, Rabat, Morocco.

Abstract: This paper addresses a new control of three phase half bridge interleaved buck shunt active power filter (HBIB-SAPF). We aim for a control strategy achieving simultaneously, the two following objectives: i) compensation of harmonic currents and reactive power absorbed by nonlinear loads for satisfying a power factor correction; ii) regulation of the HBIB converter DC capacitor voltage. To meet the above objectives, the proposed controller structure consists of two loops. The inner loop is designed using a hybrid dynamical approach to model the system, the hybrid automaton is proposed to deal with the compensation topic by switching between the different operative modes, which is conditioned by some invariance and transition conditions. The outer loop is built up based on fuzzy logic control (FLC), applied to regulate the DC bus voltage of three phase HBIB-SAPF. It is confirmed, via simulation results in Matlab/ SimPowerSystems & Stateflow toolbox that the proposed controller actually achieves the objectives it is designed for.

Keywords: Three phase HBIB-SAPF; Hybrid dynamical approach; Hybrid automata; Fuzzy logic controller; PFC.

1. INTRODUCTION

The growing use of nonlinear loads in many industrial factories has resulted in significant power quality issues into the electric power system (Hekss et al., 2019a). As one of the most perilous problems, current harmonics generated by the nonlinear loads that lead to the distortion of the voltage signal at the point of common coupling (PCC), degrade overall system efficiency and worsen power factor (PF) performances (Hekss et al., 2019b). They also disturb other consumers and interfere in nearby communication networks (Abouloifa et al., 2014)

The compensation of these harmonics are mainly done with using passive filters (Ahmed et al., 2007), due to its weaknesses such as the resonance effect, frequency tuning and the larger size (Mahela et al., 2016), active power filters (APFs) have been introduced as a proficient device to improve power quality, especially the shunt APF based on voltage source inverter (VSI) that eliminates the current harmonics as well as compensates the reactive energy, nevertheless, this conventional VSI suffers from the shoot-through problem, which is a major killer of the reliability of the inverter. In addition, it provokes the rise of temperature in the power switches and higher electromagnetic interference (EMI) (Panda et al., 2015).

Many research papers have been published to avert this phenomenon, out of which, dead time control is one, but it is not able to completely remove the shoot-through owing to the complex control method. The technology of interleaved converter became a great way to solve the above problems. Interleaved buck (IB) converter is efficient topology with the key feature of eliminating shoot-through problem without dead time effects. Besides, the reduced voltage stress, high efficiency, and low rated power devices are other advantages associated with this topology (Sun et al., 2012).

The half bridge interleaved buck (HBIB) converter is used in this paper as SAPF which offers different benefits. But its good operation strictly depends on its control strategies. In this purpose, the problem of controlling three phase HBIB-SAPF has been given a great deal of interest and various control strategies have been proposed in recent years. In (Echalih et al., 2019b), half wave control strategy was introduced to ensure the power factor and current harmonic compensation of single phase HBIB-SAPF. In (Patel and Panda, 2018), the authors present an adaptive hysteresis regulator based on $i_d - i_q$ method for three phase four-wire system which the topology of SAPF consists of three single phase full bridge interleaved buck converter, this controller is also described in (Panda et al., 2015). On the other hand, the researchers are worried to maintain the DC bus voltage constant as one of the essential aspects to the harmonic compensation performance of APFs. Hence different controllers have been used such as enhanced particle swarm optimization in (Gali et al., 2018), PI controller and FLC. Recently, fuzzy logic has been adapted and great attention has been given in their usage as no accurate mathematical model is needed as compared to another regulator (Fahmy et al., 2018).
The classical control of interleaved converters is generally processed from the average model, which is used to describe the average behavior of the converter signals during the switching period. However, this method does not show the

complete dynamics of the system, ignores high order terms in the model, and does not consider the switching characteristics of the devices. In fact, this procedure presents some difficulties in the control design of power converters. In order to cope with these systems in general, and the HBIB converter in particular, is by adopting its exact model, which is hybrid by nature due to the existence of continuous dynamics interacting with discrete events. Newly, there are increasing research interests in using a hybrid approach to model and control systems, specifically the hybrid automata theory (Echalih et al., 2019).

This paper presents a new controller for three phase half bridge interleaved buck shunt active power filter that uses the traditional two control loops decomposition. In our work, the controller inner loop is developed using hybrid automata theory. The idea is to define the control laws for different functioning modes following a set of invariance and transition conditions to ensure a satisfactory compensation of harmonic and reactive currents absorbed by the nonlinear load. The outer loop is based on fuzzy logic control to regulate the DC capacitor voltage despite load changes. The complete system with the proposed controller offers very good results, both in transient and steady-state behavior.

The paper is structured as follows: Section 2 is devoted for system description and modeling. Controller design is explained in Section 3. Simulation details, along with the results showing the effectiveness of the proposed topology and controller, is given in Section 4. Finally, the major conclusion of this paper is presented in Section 5.

2. SYSTEM DESCRIPTION AND MODELING

2.1 HBIB-SAPF Description

The schematic diagram of the proposed three phase half bridge interleaved buck converter based shunt active power filter (HBIB-SAPF) is shown in Fig. 1. It consists of six legs which configure as three single phase interleaved half bridge converter with a common DC bus. So, each leg is composed of one power IGBT and one discrete diode. The interfacing inductors (L_{1a} and L_{2a} ; L_{1b} and L_{2b} ; L_{1c} and L_{2c}) connect the HBIB converter to the grid at a point of common coupling (PCC), they also act as a medium for transferring the energy. The input of interleaved SAPF is connected with DC-link capacitor C_{dc} at the DC side. A three phase full-bridge rectifier with inductive and resistive elements (RL) load is treated as nonlinear load and connected to the grid which injects current harmonics and draws reactive power.

The grid voltage is supposed sinusoidal, and it is given by:

$$v_{gj}(t) = E_g \sin(\omega_g t - (i-1)\tfrac{2\pi}{3}); (i = 1,2,3), (j = a,b,c) \quad (1)$$

where E_g and ω_g denote, respectively, the amplitude and the angular frequency of the three phase power grid.

The load currents ($i_{La}(t)$, $i_{Lb}(t)$, $i_{Lc}(t)$), in steady-state, are periodic signals and so assume a Fourier series expansion of the form:

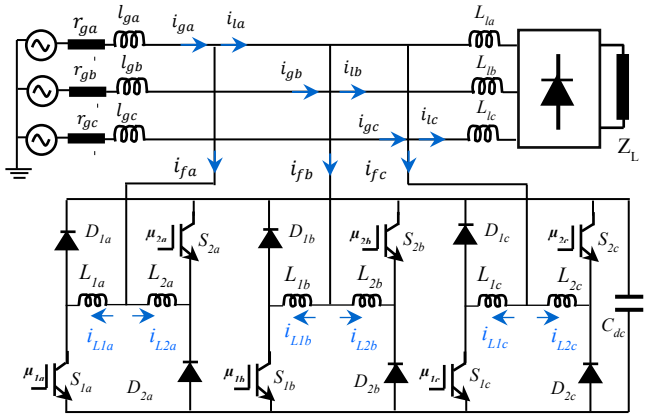

Fig. 1. 3-phase half bridge interleaved buck active power filter.

$$i_{Lj}(t) = \sum_{h=1}^{\infty} I_{j,h} \sin(h\omega_g t + \varphi_{hj}); (j = a,b,c) \quad (2)$$

where $I_{j,h}$ and φ_{hj} denote, respectively, the amplitude and the phase of the harmonic current of order h.

For this 3-phase HBIB-SAPF, the following equations are valid;

$$\begin{aligned} i_{ga} + i_{gb} + i_{gc} &= 0 \\ i_{fa} + i_{fb} + i_{fc} &= 0 \end{aligned} \quad (3)$$

where i_{ga}, i_{gb}, i_{gc} represent the respective phase grid current. Similarly i_{fa}, i_{fb} and i_{fc} represent the filter current:

$$\begin{aligned} i_{fa} &= i_{L1a} + i_{L2a} \\ i_{fb} &= i_{L1b} + i_{L2b} \\ i_{fc} &= i_{L1c} + i_{L2c} \end{aligned} \quad (4)$$

where $i_{L1a}, i_{L2a}, i_{L1b}, i_{L2b}, i_{L1c}, i_{L2c}$ are the corresponding phase coupling inductor currents.

The interleaved buck SAPF works on a different principle to the conventional VSI. The switches devices are controlled via a binary input signal $\mu_{ij} \in \{0,1\}, (\, i = 1,2; j = a,b,c)$, where two legs in each phase are operated in time opposition depending on the polarity of the phase filter current i_{fj} as described below:

$$\begin{cases} \text{if } \; i_{fj} > 0 \; then \; S_{1j} \; on, \; D_{1j}, S_{2j}, D_{2j} \; off \implies i_{fj} = i_{L1j} \\ \text{if } \; i_{fj} < 0 \; then \; S_{2j} \; on, \; S_{1j}, D_{1j}, D_{2j} \; off \implies i_{fj} = i_{L2j} \end{cases}$$

So, it never has two power switches are conducted simultaneously, there is only one active state per leg. As a result, shoot through is no longer possible.

The instantaneous model of the HBIB-SAPF is given by:

$$\frac{di_{L1j}}{dt} = \frac{1}{L_{1j}}\left[v_{gj} + v_{dc}(2\mu_{1j} - 1)\right]\gamma_j \quad (5a)$$

$$\frac{di_{L2j}}{dt} = \frac{1}{L_{2j}}\left[v_{gj} - v_{dc}(2\mu_{2j} - 1)\right](1 - \gamma_j) \quad (5b)$$

$$\frac{dv_{dc}}{dt} = \frac{1}{C}\left[-i_{L1j}(2\mu_{1j} - 1)\gamma_j + i_{L2j}(2\mu_{2j} - 1)(1 - \gamma_j)\right] \quad (5c)$$

$$\gamma_j = \tfrac{1+sgn(i_{fj})}{2}; \; sgn(i_{fj}) = \begin{cases} +1 & \text{if} \quad i_{fj}(t) > 0 \\ -1 & \text{if} \quad i_{fj}(t) < 0 \end{cases}; \; j = a,b,c \quad (6)$$

2.2 Hybrid Model

The HBIB-SAPF has a hybrid behavior characterized by the presence of continuous variables (voltages and currents) and discrete variables (states of the switches). At every phase of HBIB-SAPF, the input signals (μ_{1j}, μ_{2j}) combinations offer four different operation modes. Each functioning mode can be represented by the following affine differential equation:

$$\dot{x} = f_{qij}(x) = A_{qij}x_j + B_{qij}\,; \qquad j = a,b,c \tag{7}$$

with $x_j = \left[i_{L1j}, i_{L2j}, v_{dc}\right]^T \in X$ is the continuous state vector defined in operating region $X \subseteq \mathbb{R}^3$. $q_i \in Q$ represents the switching signal, with $Q = \{q_1, q_2, q_3, q_4\}_j$ is the set of discrete modes. For each discrete mode, the corresponding values of the inputs and the state matrices $A_{qij} \in \mathbb{R}^{3\times3}, B_{qij} \in \mathbb{R}^{3\times1}$ are given in table 1 and 2 respectively. Fig. 2 shows the specific topology obtained by the states of operating switches.

Table 1. Discrete modes of the HB-IB SAPF

Discrete modes	Input signals μ_{1j}	μ_{2j}	γ_j	Currents Evolution i_{L1j}	$\frac{di_{L1j}}{dt}$	i_{L2j}	$\frac{di_{L2j}}{dt}$
q_{1j}	1	0	1	>0	>0	0	0
q_{2j}	0	0	1	>0	<0	0	0
q_{3j}	0	0	0	0	0	<0	<0
q_{4j}	0	1	0	0	0	<0	>0

Table 2. State matrices for operating modes

modes	A_{ij}	B_{ij}
q_{1j}	$\begin{bmatrix} 0 & 0 & \frac{1}{L_{1j}} \\ 0 & 0 & 0 \\ \frac{-1}{C} & 0 & 0 \end{bmatrix}$	$\begin{bmatrix} \frac{v_{gj}}{L_{1j}} \\ 0 \\ 0 \end{bmatrix}$
q_{2j}	$\begin{bmatrix} 0 & 0 & \frac{-1}{L_{1j}} \\ 0 & 0 & 0 \\ \frac{1}{C} & 0 & 0 \end{bmatrix}$	$\begin{bmatrix} \frac{v_{gj}}{L_{1j}} \\ 0 \\ 0 \end{bmatrix}$
q_{3j}	$\begin{bmatrix} 0 & 0 & 0 \\ 0 & 0 & \frac{1}{L_{2j}} \\ \frac{-1}{C} & 0 & 0 \end{bmatrix}$	$\begin{bmatrix} \frac{v_{gj}}{L_{2j}} \\ 0 \\ 0 \end{bmatrix}$
q_{4j}	$\begin{bmatrix} 0 & 0 & 0 \\ 0 & 0 & \frac{-1}{L_{2j}} \\ \frac{1}{C} & 0 & 0 \end{bmatrix}$	$\begin{bmatrix} \frac{v_{gj}}{L_{2j}} \\ 0 \\ 0 \end{bmatrix}$

3. CONTROL SYSTEM DESIGN

3.1 Control Objectives

In this section, our aim is to design for HBIB-SAPF a controller that will be able to guarantee the two main objectives mentioned previously: (i) Power factor correction (PFC), (ii) a tight regulation of the converter DC bus capacitor voltage. The used structure is based on two loops: current inner loop and voltage outer loop, as shown in the schematic diagram in Fig. 3.

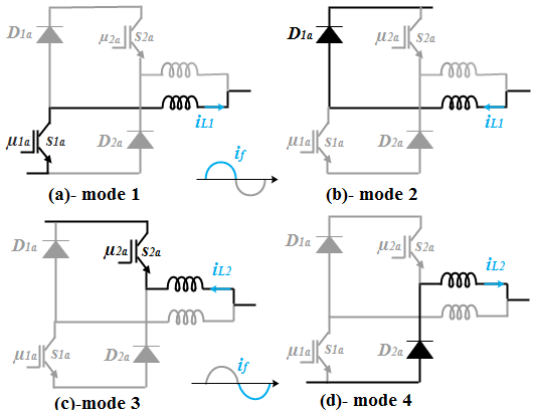

Fig. 2. Operation phase-a of HBIB SAPF.

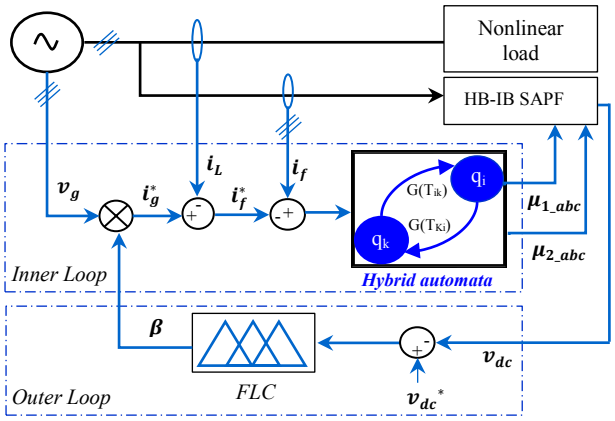

Fig. 3. The structure of controller.

3.1 Current Inner Loop

The inner loop current controller is constructed to ensure the unity power factor. It means that the three phase grid current $\left[i_{ga}\ i_{gb}\ i_{gc}\right]^T$ must be sinusoidal and in phase with the grid voltage $\left[v_{ga}\ v_{gb}\ v_{gc}\right]^T$. So, this goal is achieved indirectly by forcing the current $i_{f(abc)}$ injected by the filter to follow the best as possible the reference signal defined by:

$$\begin{bmatrix} i_{fa}^* \\ i_{fb}^* \\ i_{fc}^* \end{bmatrix} = \beta \begin{bmatrix} v_{ga} \\ v_{gb} \\ v_{gc} \end{bmatrix} - \begin{bmatrix} i_{La} \\ i_{Lb} \\ i_{Lc} \end{bmatrix} \tag{8}$$

β is a positive real signal fixing the amplitude of the current.

- Hybrid Automaton

The HBIB-SAPF is presented as a hybrid system. Therefore, the hybrid automaton is developed to switch from one operating mode to another in order to control the system. Indeed, the hybrid automaton appears as a finite state machine with a finite set of continuous variables that described by ordinary differential equations. The whole system can be defined by the following hybrid formalism (Lunze and Lamnabhi Lagarrigue, 2009).

$$H = \{\, Q, X, f_q, I_q, T, G, Init \,\} \tag{9}$$

f_q: $Q \times X \rightarrow \mathbb{R}^n$ assigns to every discrete mode a continuous dynamic given by (7); I_q: $Q \rightarrow 2^X$ associates an invariant field for the discrete state q; $T \subset Q \times Q$ is the set of possible transitions in the automaton; $G : T \rightarrow 2^X$ is the constraint in the continuous field for validating a transition, is also called the guard condition; $Init \subseteq X \times Q$ gives the initial states.

Fig. 4 illustrates the hybrid automaton for the HBIB-SAPF. The dynamics of each mode is indicated inside each circle. The transition conditions $G_{ij}; (j = a, b, c)$ between the different modes are drawn above the arrows to represent the commutation constrained by the verification of the switching conditions.

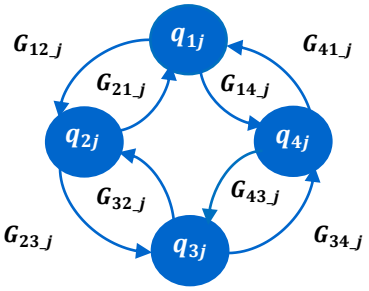

Fig. 4. Hybrid automaton of the HBIB-SAPF.

- Invariances and Transition Conditions

According to table 1, the transition and invariance conditions are defined to force the system to switch between operation modes in order to track the desired reference zone for the filter current, which allows reaching the first objective, i.e. the unity power factor. Indeed, each mode is characterized by current error (either positive or negative). Thus, based on the measured filter current i_{fj} injected by HBIB-SAPF, the algorithm switches to an adequate mode from the admissible set in order to ensure that the filter current follows its reference.

The invariance conditions I_{qij} {i = 1, 2, 3, 4; j = a, b, c} for each mode q_{ij} are defined as follows:

$$I_{q1j} = \left\{ [i_{fj} > 0] \wedge \left[\frac{di_{fj}}{dt} > 0\right] \wedge (i_{fj} - i_{fj}^*) \leq -\varepsilon \right\}$$

$$I_{q2j} = \left\{ [i_{fj} > 0] \wedge \left[\frac{di_{fj}}{dt} < 0\right] \wedge (i_{fj} - i_{fj}^*) \geq +\varepsilon \right\}$$

$$I_{q3j} = \left\{ [i_{fj} < 0] \wedge \left[\frac{di_{fj}}{dt} < 0\right] \wedge (i_{fj} - i_{fj}^*) \leq -\varepsilon \right\}$$

$$I_{q4j} = \left\{ [i_{fj} < 0] \wedge \left[\frac{di_{fj}}{dt} > 0\right] \wedge (i_{fj} - i_{fj}^*) \geq +\varepsilon \right\}$$

The guard conditions corresponding to the convergence of the three phase filter current to their references are defined by the conditions of transition $G(T_{ik\_j}) = G(q_i, q_k)_j$ between the operating mode q_i to the mode q_k, for $\{i, k = 1, 2, 3, 4\}$, which are expressed as follows:

$$G(q_1, q_2)_j = \{x \in X | \, (i_{fj} - i_{fj}^*) \geq +\varepsilon\}$$

$$G(q_2, q_1)_j = \{x \in X | \, (i_{fj} - i_{fj}^*) \leq -\varepsilon\}$$

$$G(q_2, q_3)_j = \{x \in X | \; i_{fj} < 0\}$$

$$G(q_3, q_2)_j = \{x \in X | \; i_{fj} > 0\}$$

$$G(q_3, q_4)_j = \{x \in X | \, (i_{fj} - i_{fj}^*) \geq +\varepsilon\}$$

$$G(q_4, q_3)_j = \{x \in X | \, (i_{fj} - i_{fj}^*) \leq -\varepsilon\}$$

$$G(q_1, q_4)_j = \{x \in X | \; i_{fj} < 0\}$$

$$G(q_4, q_1)_j = \{x \in X | \; i_{fj} > 0\}$$

The initial conditions of the system are defined by:

$$init = \{q_1\} \times \left\{x \in X | \, (i_{fj} > 0) \wedge \left(\frac{di_{fj}}{dt} > 0\right)\right\}.$$

3.3 Voltage Outer Loop

The aim of this loop is to generate a signal β in order to regulate the output voltage v_{dc} to a given reference value v_{dc}^*. Here the fuzzy logic controller (FLC) has been used for the DC-link voltage regulation system due to its own advantages as compared to a conventional linearized model based PI controller.

The proposed fuzzy logic controller for regulating the HBIB-SAPF DC voltage is shown in Fig. 5, whose inputs are the error voltage ($\varepsilon(n) = v_{dc}^*(n) - v_{dc}(n)$) and its variation ($\Delta\varepsilon(n) = \varepsilon(n) - \varepsilon(n-1)$) at n^{th} sampling instant. The output of the FLC is the signal β. Coefficient G is used to adjust the estimation. The fuzzy control system is composed of three different stages: Fuzzification, rules execution, and defuzzification.

- Fuzzification: is the process of converting crisp values of the input variables to an analogous linguistic variable based on certain membership function (MF).
- The rule base is the principal component of the fuzzy controller; it indicates how the controller behaves to response to any input situation. The rules execution is constituted a collection of (IF-THEN).
- Defuzzification: is the progression of converting back the fuzzy output into a crisp numerical value.

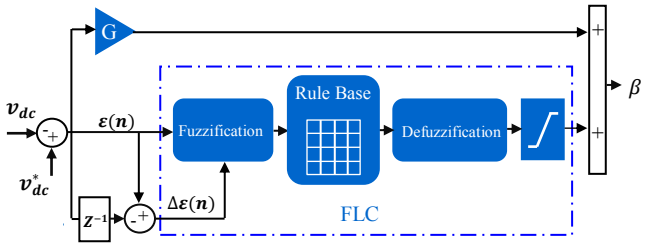

Fig. 5. Fuzzy controller structure.

- Basic Fuzzy Algorithm

The Mamdani fuzzy inference system (*FIS*) was selected for use in this study. So, its characteristics comprise of seven triangular membership functions to describe each input i.e. $\varepsilon(n)$, $\Delta\varepsilon(n)$ and the output, the corresponding fuzzy sets are chosen as *NB= Negative Big*, *NM= Negative Medium*, *NS= Negative Small*, *Z= Zero, PS= Positive Small*, *PM= Positive Medium*, *PB= Positive Big*, are shown in Fig. 6. The processed method called fuzzification is being implemented by Universe of Discourse (UOD), implication using "min" operator, aggregation by "max" operator. Finally, defuzzification has been carried out using the "centroid of area (COA)" method.

- Design of Control Rules

The fuzzy control design involves defining rules that relate the input variables to the output model properties. For better control performance, smaller fuzzy partitioned subspaces are used and summarized in table 3. The elements of this rule base are determined based on the theory that in the transient state, large errors need coarse control, which involves coarse input/output variables, while in the steady-state, small errors need fine control which involves fine input/output variables.

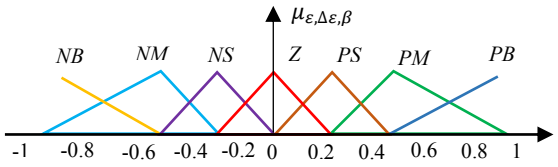

Fig. 6. Membership functions of input and output variables.

Table 3. Rules base for fuzzy controller

ε / $\Delta\varepsilon$	NB	NM	NS	Z	PS	PM	PB
NB	NB	NB	NB	NB	NM	NS	Z
NM	NB	NB	NB	NM	NS	Z	PS
NS	NB	NB	NM	NS	Z	PS	PM
Z	NB	NM	NS	Z	PS	PM	PB
PS	NM	NS	Z	PS	PM	PB	PB
PM	NS	Z	PS	PM	PB	PB	PB
PB	Z	PS	PM	PB	PB	PB	PB

5. SIMULATION RESULTS

To evaluate the performance of the proposed controller, Matlab/SimPowerSystems & Stateflow toolbox are used to model the instantaneous circuit dynamics of the system as well as the control scheme. The system parameters are shown below:

$v_g = 230V, f_g = 50HZ,\ r_g = 0.1\Omega,\ l_g = 0.2\mu H.$
$R_1 = 15\,\Omega,\ R_2 = 30\Omega,\ L = 500\,mH, L_{lj} = 1mH.$
$\mathrm{C} = 1mF, L_{fj} = 6mH,\ v_{dc}^* = 900V.$

The steady-state and the transient performances have been tested for the proposed controller under nonlinear load, which is formed using three phase full-wave diode bridge rectifier with resistive and inductive elements (R-L load).

5.1 Steady-State Performance

Figs. 7-12 show the results of simulation, which are selected to demonstrate the most significant aspect of the system behavior. Fig. 7 illustrates the three phase load current waveform i_{Labc} that is much distorted where its harmonic spectrum found to be 24.84%. Fig. 8. shows that the filter current injected in the grid converges to its reference signal with a good accuracy. Fig.9 depicts the obtained three phase grid current, where a zoom for phase-a is illustrated in Fig. 10, it shows that the grid current is sinusoidal and in phase with the grid voltage. As a result, a unity power factor is attained. Fig. 11 shows the result of DC voltage regulation based on fuzzy logic control (FLC). It is contemplated that the DC bus voltage set at its required reference value, which is equal to 900V. Fig. 12 shows the β signal that represents the output signal of the fuzzy logic controller.

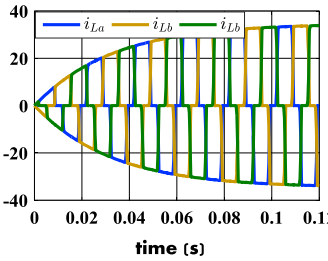

Fig. 7. 3-phase load current.

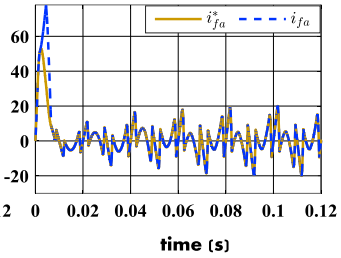

Fig. 8. Filter current phase-a.

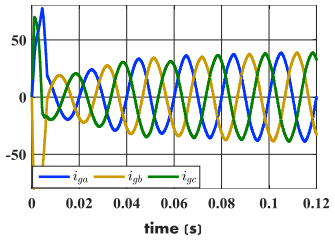

Fig. 9. 3-phase grid current.

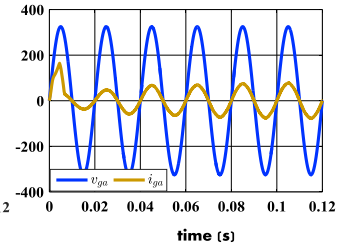

Fig. 10. PFC checking.

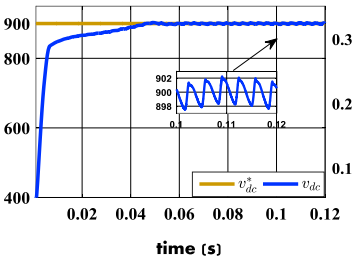

Fig. 11. Dc bus voltage v_{dc}.

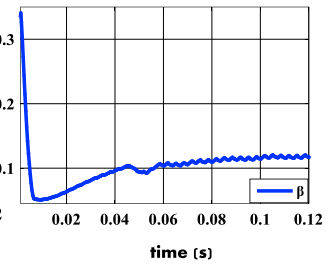

Fig. 12. Signal β.

5.2 Transient State Performance

To analyze the robustness capability of the proposed controller, a new simulation trial will be performed. It involves changing the load resistance according to Fig. 13. Except for this change, the rest of the system characteristics are similar as previously. Figs. 14-17 illustrate the resulting controller behavior. It is seen from Fig. 14 that the disturbing effect of the load changes is well compensated by the fuzzy logic controller. The DC-link capacitor voltage is recovered and achieves its reference v_{dc}^* after a transient time of 0.1s with small ripples. This is also demonstrated in Fig. 15 where the outer-loop control β gets constant after load change. Fig. 16 shows the load current i_{Labc} in the presence of varying load resistance. Fig. 17 shows that the grid current i_{gabc} remains sinusoidal all the time and in phase with the grid voltage, this proves that the proposed controller shows the good compensation performance. Table 4 summarizes the THD values of the mitigated grid current in the steady and transient state conditions. We can see that the THD is reduced below 5%, which conforms to the limit set by IEEE.

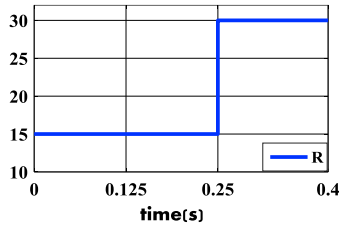

Fig. 13. Load change.

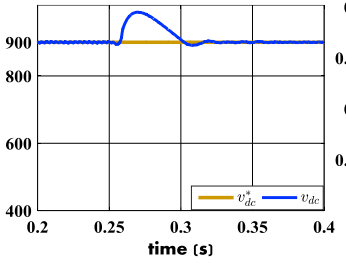

Fig. 14. Dc bus voltage v_{dc}.

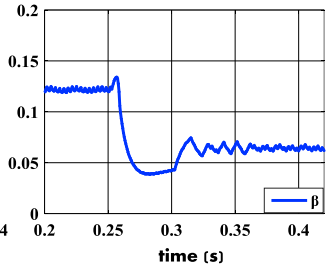

Fig. 15. Signal β.

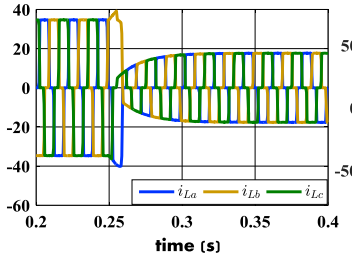

Fig. 16. Load current i_{Labc}.

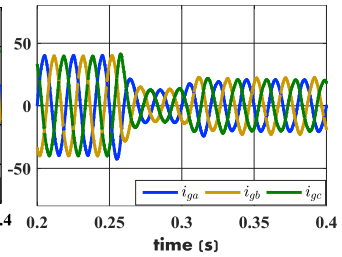

Fig. 17. Grid current i_{gabc}.

Table 4. THDs of Mitigated Grid Current

Total Harmonic Distortion, (THD %)	
Bridge R_1L	***Bridge R_2L***
Before connecting HBIB-SAPF	
24.94%	*28.24%*
After connecting HBIB-SAPF	
1.18%	*1.90%*

6. CONCLUSION

This work has presented the problem of controlling the three phase interleaved buck shunt active power filter using the traditional double loop. Thanks to the hybrid nature of the half bridge interleaved buck converter, a hybrid automaton has been designed in the inner loop to control the system by switching between different functioning modes in order to compensate the harmonic currents and reactive energy absorbed by the nonlinear load. The outer loop is designed to ensure the regulation of the DC capacitor voltage, using the fuzzy logic control. From the obtained results, it is proved that the shoot-through problem gets eliminated, improving the reliability of the active power filter. Again, the THD of the grid has been drastically brought down to less than 5% as required. Moreover, the proposed controller shows the fast-tracking and a good robustness against DC bus voltage variation.

REFERENCES

Abouloifa, A. Giri, F. Chaoui, F.Z. Kissaoui, M. and Abouelmahjoub. Y. (2014). Cascade nonlinear of shunt active power filters with average performance analysis. *Control Eng. Pract*, volume (26), p. 211-221.

Ahmed, K.H. Finny, S.J. and Williams, B.W. (2007). Passive filter design for three-phase inverter interfacing in distributed generation. In Compatibility in power Electronics (CPE), 2007, p. 1-9.

Echalih, S. Abouloifa, A. Lachkar, I. Hekss, Z. Aourir, M. and Giri, F. (2019). Hybrid control of single phase shunt active power filter based on interleaved buck converter. In 2019 American Control Conference (ACC). IEEE, 2019, p. 3636-3641.

Echalih, S. Abouloifa, A. Hekss, Z. and Lachkar, I. Half wave control strategy of interleaved buck converter based single phase active power filter for power quality improvement. 2019 4th World Conference on Complex Systems (WCCS), Ouarzazate, Morocco, 2019, p. 1-6.

Fahmy, A. M. Abdelslam, A.K. Ahmed. K. Lotfy, A.A. Hamad, M. and Kotb, A. (2018). Four leg shunt active power filter predictive fuzzy logic controller for low-voltage unbalanced load distribution networks. *Journal of Power Electronics*, 18 (2), p. 573-587.

Gali, V. Gupta, N. and Gupta, R.A. (2018). Enhanced particle swarm optimization based DC link voltage control algorithm for interleaved SAPF. *Journal of engineering science and technology*. 13 (10), p. 3393-3418.

Hekss, Z. Lachkar, I. Abouloifa, A. Echalih, S. Aourir, M. and Giri, F. (2019). Nonlinear control strategy of single phase half bridge shunt active power filter interfacing renewable energy source and grid. In 2019 American Control Conference (ACC). IEEE, 2019, p. 1971-1976.

Hekss, Z. Abouloifa, A. Echalih, S. and Lachkar, I. Cascade nonlinear control of photovoltaic system connected to single phase half bridge Shunt Active Power Filter. 2019 4th World Conference on Complex Systems (WCCS), Ouarzazate, Morocco, 2019, p. 1-6.

Lunze, J., and Lamnabhi-Lagarrigue, F. (2009). *Handbook of hybrid systems control: theory, tools, applications*. Cambridge University Press.

Mahela, O.P. and Shaik, A.G. (2016). Topological aspects of power quality improvement techniques: A comprehensive overview. *Renewable and Sustainable Energy Reviews*, (58), p. 1129-1142.

Panda, A.K. Patel, R. and Patnaik, N. (2015). 3-phase 4-wire h-bridge interleaved buck shunt active power filter using real time simulator. In Proceeding INDICON, 2015 Annual IEEE, New Delhi, p. 1-6.

Patel, R. Panda, A.K. (2018). Real-time harmonic mitigation using Fuzzy based highly reliable three dual buck full bridge APF for dynamic unbalanced load. *International Journal of Emerging Electric Power Systems*, 19(3).

Sun, P.W. Liu, C. Lai, J.S. Chen, C.L. Kees, N. (2012). Three phase dual buck inverter with unified pulsewidth modulation. *IEEE Trans. Power Electron*, 27 (3), p. 1159-1167.